Environmental Research 214 (2022) 114088

Contents lists available at ScienceDirect

Environmental Research

journal homepage: www.elsevier.com/locate/envres

Environmental microplastics (EMPs) exposure alter the differentiation potential of mesenchymal stromal cells

Hana Najahi [a,b], Nicola Alessio [c], Tiziana Squillaro [c], Gea Oliveri Conti [d], Margherita Ferrante [d], Giovanni Di Bernardo [c], Umberto Galderisi [c], Imed Messaoudi [b], Sergio Minucci [c], Mohamed Banni [a,b,*]

[a] *Laboratory of Agrobiodiversity and Ecotoxicology LR21AGR02, Sousse University, Chott-Mariem, 4042, Sousse, Tunisia*
[b] *Higher Institute of Biotechnology, Monastir University, Tunisia*
[c] *Department of Experimental Medicine, "Luigi Vanvitelli" Campania University, 81038, Napoli, Italy*
[d] *Environmental and Food Hygiene Laboratory (LIAA), Department of Medical, Surgical Sciences and Advanced Technologies G. F. Ingrassia, Catania University, Via Santa Sofia 87, 95123, Catania, Italy*

ARTICLE INFO

Keywords:
Mesenchymal stromal cells
EMPs
PET
Differentiation stem cells
Senescence

ABSTRACT

Humans are exposed to environmental microplastic (MPs) that can be frequent in surrounding environment. The mesenchymal stromal cells are a heterogeneous population, which contain fibroblasts and stromal cells, progenitor cells and stem cells. They are part of the stromal component of most tissue and organs in our organisms. Any injury to their functions may impair tissue renewal and homeostasis. We evaluated the effects of different size MPs that could be present in water bottles on human bone marrow mesenchymal stromal cells (BMMSCs) and adipose mesenchymal stromal cells (AMSCs). MPs of polyethylene terephthalate (MPs-PET) (<1 μm and <2.6 μm) were tested in this study. PET treatments induced a reduction in proliferating cells (around 30%) associated either with the onset of senescence or increase in apoptosis. The AMSCs and BMMSCs exposed to PET showed an alteration of differentiation potential. AMSCs remained in an early stage of adipocyte differentiation as shown by high levels of mRNA for Peroxisome Proliferator Activated Receptor Gamma (*PPARG)* (7.51 vs 1.00) and reduction in Lipoprotein Lipase (*LPL)* mRNA levels (0.5 vs 1.0). A loss of differentiation capacity was also observed for the osteocyte phenotype in BMMSCs. In particular, we observed a reduction in Bone Gamma-Carboxy glutamate Protein (BGLAP) (0.4 for PET1 and 0.6 for PET2.6 vs 0.1 CTRL) and reduction in Osteopontin (SPP1) (0.3 for PET 1 and 0.64 for PET 2.6 vs 0.1 CTRL).

This pioneering mesenchymal cell response study demonstrated that environmental microplastic could be bioavailable for cell uptake and may further lead to irreversible diseases.

1. Introduction

Each year, over 8 million tons of plastic gets dumped into the environment, both on land and in the sea. Indeed, the world plastic production has skyrocketed nearly 200 times in the last years (Jambeck et al., 2015). Nevertheless, consumption is still growing exponentially.

The definition of microplastics (MPs), was first reported by Tompson in 2004 and designates very small plastic particles and plastic fibers having a diameter less than 5 mm. MPs also include nanoplastics (NPs), whose diameters are below 0.1 μm (100 nm). Due to their small size, MPs can be potentially dangerous, since they can be easily absorbed by the organism's tissues and organs (Fournier et al., 2021). Nevertheless, MPs are used in certain industries.

MPs are classified as primary and secondary. Primary MPs have industrial use, and they are among the raw materials for certain consumer products too, while secondary MPs are those that are derived from the decomposition of macroplastics due to the different processes of environmental mechanical degradation, biodegradation and chemical degradation (Oliveira et al., 2020).

As MPs persistently remain in the environment, they accumulate in organisms (Oliveri Conti et al., 2020), especially in marine ecosystems (Ferrante et al., 2021). In this context, the marine living species are a major contamination source (Cappello et al., 2021; De Marco et al., 2022; Missawi et al., 2022; Zitouni et al., 2022). Humans can be MPs

* Corresponding author. Laboratory of Agrobiodiversity and Ecotoxicology LR21AGR02, Sousse University, Chott-Mariem, 4042, Sousse, Tunisia.
E-mail address: mohamedbanni414@gmail.com (M. Banni).

https://doi.org/10.1016/j.envres.2022.114088
Received 8 June 2022; Received in revised form 5 August 2022; Accepted 6 August 2022
Available online 13 August 2022
0013-9351/

exposed by several routes: inhalation, food and skin. For these reasons, in recent years, research has been carried out with a focus on the human health risks of MPs exposure (Kannan and Vimalkumar., 2021).

A recent study demonstrated the presence of plastic particles in human bloodstream (Leslie et al., 2022) thus providing robust proofs of the occurrence of plastic contamination in human body. Moreover, studies involving humans have shown the transfer of MPs through the intestine to the lymphatic system (Kannan and Vimalkumar, 2021). This transfer is even more highlighted in the colon of patients with inflammatory bowel disease, which correlates with an increase in intestinal permeability (Bredeck et al., 2021; Kannan and Vimalkumar, 2021). The presence of MPs in the intestine can be toxic due to its intrinsic ability to induce intestinal blockages or tissue abrasions (Kannan and Vimalkumar, 2021). Furthermore, the passage of MPs to the lymphatic system suggests that they can reach any part of an organism. This is due also to another worrying aspect, i.e., their microscopic size; in fact, MPs and NPs could find different paths of absorption either by phagocytosis or endocytosis (Guerrera et al., 2021).

Mesenchymal Stromal Cells (MSCs), residing in the bone marrow (BM), adipose tissue (AT), and in the stromal component of other tissues, are made of subpopulation of stem cells that can differentiate in chondrocytes, osteocytes, adipocytes, and smooth muscle cells. In addition, MSCs sustain hematopoiesis process, support the organismal homeostasis, and regulate the inflammatory response. MSCs also have a crucial therapeutic value (Galderisi and Giordano, 2014). The valuable effect of MSCs in homeostasis and tissue repair occurs through the secretion of many factors. The presence of MSCs in the BM of skeletal bones and in the AT, which is widely distributed in human body (beneath the skin, between muscles, around the kidneys, heart, and abdominal membranes) increases the possibility to suffer from genotoxic damage, including exposure to MPs (Ferrante et al., 2021). As a result of their long lifespan, stem cells can undergo multiple rounds of damage, MPs that individually do not have a major impact on cell physiology, but collectively can severely impair cell function.

In view of the afore said factors, we hypothesized that neither the microenvironment of the BM nor the AT that is a dense vascular network are safe from being penetrated by MPs (Herold and Kalucka, 2020).

For these reasons, we hypothesized that the highly vascularized tissues such as BM and AT are not immune to this phenomenon. The present study aims to analyze the effects of MPs-PET of different sizes (1 and 2.6 μm) on human BM mesenchymal stromal cells (BMMSCs) and adipose mesenchymal stromal cells (AMSCs). We evaluated the effects of MPs-PET on the biology of MSCs in terms of the cell cycle, senescence and apoptosis, focusing our attention on their differentiation capacity.

2. Materials and methods

2.1. Human bone marrow and adipose MSCs

The human BMMSCs (Catalog #: 2M-302) and AMSCs (Catalog #: PT-5006) were obtained by Lonza (CH) and cultivated according to manufacturer's instruction. In details, MSCs were seeded 1 to 2.5 × 10^5 cells/cm^2 in a growth medium that contains alpha-minimum necessary medium (αMEM) (EuroClone, Napoli, Italy) containing 10% fetal bovine serum (FBS) (EuroClone, Napoli, Italy) and 3 ng/ml basic fibroblast growth factor (β-FGF) (Preprotech, London, UK). After Over Night (ON), the non-adherent cells were discarded, and adherent cells were cultivated, when they reached 70%–80% confluence, the cells have been harvested by the usage of Trypsin-EDTA (EuroClone, Napoli, Italy) and subcultured at 1:3 dilution.

2.2. Preparation of MPs

The MP particles derived from uncolored PET water bottles. The polymer type was verified by FTIR spectroscopy (FTIR, Thermo Scientific, MS, USA). In brief, a bottle sample (10 g) was flash-frozen with liquid nitrogen and then grounded in a swing mill to obtain irregular particles having heterogeneous form and size. The obtained samples were filtered with a 30 μm sieve and then diluted in 100 ml of MQ water. The obtained plastic dust was successively filtered through small pores of cellulose nitrate filters (Ø = 47 mm, 2.67 μm, and 1 μm) (Healthcare Life Science, UK) to obtain two solutions with two size ranges of MPs (2.67–1 μm and under 1 μm). These two size ranges were selected for this study because they are the most abundant in packaged waters (Zuccarello et al., 2019). We performed a Scanning Electron Microscopy qualitative analysis ofthe particle surface structure (Cambridge Instruments, UK - Mod. Stereoscan 360). The microscopy analysis was associated with SEM-EDX (X Energy Dispersion Detector) using the Inca software. The SEM-EDX was also used to count the number of particles per ml for each size range and further transformed to μg/L based on PET density (Zuccarello et al., 2019).

2.3. MSC treatment with PET and proliferating assay

For an evaluation of PET effects on *in-vitro* MSC functions, the cells were incubated for 72 h in αMEM containing Fetal Bovine Serum (FBS; 10%), Fibroblast Growth Factor 2 (FGF2; 3 ng/ml) and PETs (10 μg/ml). Two different sizes <1 μm (PET1) and <2.6 μm (PET2.6) were used. After 72 h, the cultures were used for the programmed experiments. Cell proliferation was determined by CCK-8(Colorimetric Cell Counting) assay by Dojindo (MD, USA) according manufacturer's instruction. The water-soluble tetrazolium salt, WST-8, can be reduced by dehydrogenase in cells to produce an orange formazan dye that is soluble in the medium. The quantity of formazan dye produced by dehydrogenase exercise in the cellphone is proportional to the number of cells. In detail, after treatment with MPs, 1000 cells have been seeded per wells. Thereafter, CCK-8 had been added and at 24 h, 48 h and 72 h were assayed the viability at 450 nm by the use of a microplate reader.

2.4. Immunocytochemistry and senescence-associated β-galactosidase

After PETs exposure, the cells grown in 24 multi-wells were fixed in a 2% formaldehyde solution for 10 min. Cells were then stained for detecting Senescence-Associated Beta-Galactosidase as already reported (Alessio et al., 2015).

Following senescence staining, cells were permeabilized with 0.3% Triton-X100 (Roche, CH) and further incubated at room temperature in a blocking solution made of 0.1% Triton-X100 and 5% FBS. The samples were then incubated with the antibodies against pRPS6 (Cell Signaling, MA, USA, code 4858) and Ki67 (Santa Cruz Biotechnology, CA, USA, code sc7846) at 4 °C overnight. Goat anti-rabbit antibody (FITC-conjugated) secondary antibody (Immuno-Reagents NC, USA) and a goat anti-mouse antibody (TRITC-conjugated) secondary antibody (Immuno-Reagents (NC, USA) were used. DAPI staining was employed to recognize nuclei and images were obtained using a DM2000 Leica fluorescence microscope, For each analyzed marker, the percentage of positive cells was calculated as reported by Alessio et al. (2021).

2.5. Immunocytochemistry (ICC) for detection of ataxia-telangiectasia mutated kinase (ATM) and gamma-H2AX and DCF-DA assay

The ICC procedure was performed according our previous published method (Alessio et al., 2015). Briefly, cells were fixed in 4% formaldehyde (Sigma-Aldrich) solution for 15 min after MPs-PET exposure incubated at room temperature (RT) (20–23 °C). The cells were permeabilized cells with 0.3% Triton-X100 (Roche, Basel, Switzerland) for 5 min on ice, followed by blocking solution (5% FBS in PBS and 0.1% Triton-X100) for 1 h at RT. Subsequently, the antibodies pATM (ab36810, ABCAM, Cambridge, UK) and gamma-H2AX (2577, Cell Signaling Technology, Danvers, MA, USA) have been detected in accordance to the respective manufacturer's protocol. FITC-conjugated secondary antibodies had been bought from Immuno-Reagents

(Raleigh, NC, USA). Nuclear staining was once performed the usage of DAPI mounting medium (ab104139, ABCAM) and photomicrographs have been taken beneath a fluorescence microscope (Leica DM 2000, -DMC5400, Leica, Wetzlar, Germany). The percentages of ATM and gamma-H2AX cells have been calculated by counting at least 300 cells in different microscopic fields.

Reactive oxygen species (ROS) were evaluated by intracellular conversion of fluorescent DCFH-DA (2,7-dichlorodihydrofluorescein). Cells were incubated with 0.1% Pluronic F-127 and DCFH-DA (2 μM) for 30 min at 37 °C, then were PBS washed analyzed with easyCyte™ flow cytometer (Millipore, MS,USA) with easyCyte™ software.

2.6. Annexin-V assay

Apoptotic cells were identified with a fluorescein-conjugated Annexin V kit (Millipore, MS, USA) on a Guava easyCyte cytometer following the manufacturer's instructions. We grouped together early and late apoptotic cells.

2.7. Colony forming units assay (CFU)

Following treatments with MPs, 1,000 cells were seeded in 100 mmplate and incubated in a growth medium for 14 days according our previous published procedure (Alessio et al., 2015).

2.8. Spontaneous differentiation

MSC cultures were trypsinized after being treated with MPs and 1.5 $\times$ 10^4 cells were seeded in six-well plates pre-coated with gelatin solution (Sigma Aldrich, MO, USA). Cells were incubated in αMEM medium supplemented with 10% FBS for 21 days.

2.9. In-vitro differentiation and staining

After being treatment with MPs, 1.5 $\times$ 10^4/cm^2 cells were seeded and cultivated either in osteogenic or chondrogenic or adipogenic medium at 37 °C for 21 days as already reported (Alessio et al., 2018a,b). Cell staining for detecting osteocytes, adipocytes and chondrocytes was performed as previously described (Alessio et al., 2018).

2.10. Western blotting

Cells were lysed in buffer containing 0.1% Triton-X100 (Roche, CH) and analyzed for western blot as already reported (Alessio et al., 2017). The following primary antibodies were used: RB2/P130 from BD Biosciences (CA, USA); P27KIP1 and RB1 from Cell Signaling Technology (MS, USA), P107 (code sc-318), P53 (code DOI-1), and P21CIP1 (code C-19) from Santa Cruz Biotechnology (CA, USA); P16INK4A from ABCAM (UK).

2.11. Soft agar

After being treated with MPs, 2,500 cells were incubated in 0.5 ml DMEM containing agarose plus FBS in 35 mm Petri dishes and incubated for 21 days as already reported (Alessio et al., 2015).

2.12. Statistical analysis

Statistical significance was processed using the one-way test ANOVA followed by post hoc test (Tukey test). All data were analyzed usingthe statistical software package GraphPad Prism version 5.01 (GraphPad, CA, USA).

3. Results

3.1. Effects of PET on the MSC biology

MPs used for this study were obtained from uncolored PET water bottles. We exposed the AMSC and BMMSC cultures to MPs for 72 h. Then, we assessed the effect of MPs on the biological properties of MSCs such as: proliferation rate, cell cycle, apoptosis, and senescence. The culture exposure to different sizes of MPs showed modification in the MSC proliferation rate only for PET 2.6 μm (Fig. 1a). We also carried out ICC to identify the percentage of cycling cells (SA-β-gal-, Ki67 +, pRPS6 +). We evidenced a reduction in the cycling cells in all of the analyzed conditions (Fig. 1b). These results are in line with the cell cycle analysis (Fig. 1c), where the level of cells in S phase decreased in both AMSCs and BMMSCs after being treated with PET 1 μm and 2.6 μm (hereinafter indicated as PET1 and PET2.6, respectively).

We then performed cytochemistry analysis for SA -β-gal together with Ki67 and pRPS6 immunodetection to specifically identify senescent cells, which are SA -β-gal (+), Ki67(−), and pRPS6(+) (Alessio et al., 2021).

The percentage of senescent cells (Fig. 1d) showed an increase in BMMSC and AMSC cultures incubated with PET1, while PET2.6 treatment showed an increase in senescence only forBMMSCs.

The analysis of apoptosis, instead, showed an increase in apoptosis in AMSCs treated with PET 2.6 (Fig. 1e). The PET2.6 genotoxic damages may be more severe in AMSCs, since in these samples we detected cell death.

We then studied the molecular signaling circuits associated with PET-induced senescence and/or apoptosis. We analyzed the levels of key proteins (P53- RB-pathways) involved in these phenomena. In most of the analyzed conditions, we detected an upregulation of P27^{KIP1}, P21^{CIP1}, and P16^{INK4A}, which are cyclin kinase inhibitors (CKIs) (Fig. 1f). In detail, in samples with increased senescence we observed the upregulation of all three reported CKIs, while in AMSCs treated with PET2.6 the apoptosis onset appeared related mainly to P21^{CIP1} increase.

3.2. PET induce modification in DNA damage repair (DDR)

In recent study Chang-Bum et al. (2020) showed that the MPcellular toxicity mainly depends on oxidative stress via reactive oxygen species (ROS). This event may contribute to the senescence and apoptosis we observed following MSC treatment with MPs-PETs. ROS may induce macromolecule damages, including DNA.

For these reasons, we determined the intracellular ROS levels after MPs exposure. MPs-PET1 treatment induced an increase of ROS level in BMMSCs and AMSCs (Fig. 2a), while MPs-PET 2.67 induced ROS increase only in BMMSCs. We also evaluated the percentage of stressed cells by immunocytochemistry against Ki67, p-RPS6, and β-Gal positive cells. The results highlight that only MPs-PET1 is able to induce a stress phenotype in BMMSCs (Fig. 2b).

There are evidences that suggests that persistent DNA damage leads to increased senescence and/or apoptosis. We evaluated the persistent of damage DNA in BMMSC and AMSCS after 48 h of MPs-PET treatments with pHA2. X and pATM. We observed an accumulation of damaged DNA foci in all the experimental conditions (Fig. 2c and d). This result was in line with senescence phenomena we above reported. In order to have a clear insight on MPs-PET effects on MSCs we also evaluated the occurrence of neoplastic transformation, since recent studies suggest a link between microplastics and cancer risk. Transformed cells can grow independently of a solid surface. This feature is a typical carcinogenesis hallmark and was examined by soft agar colony formation assay. Cells cultured with MPs-PET for 48 h and matched controls showed no anchorage-independent growth until 21 days after exposure (Fig. 2e).

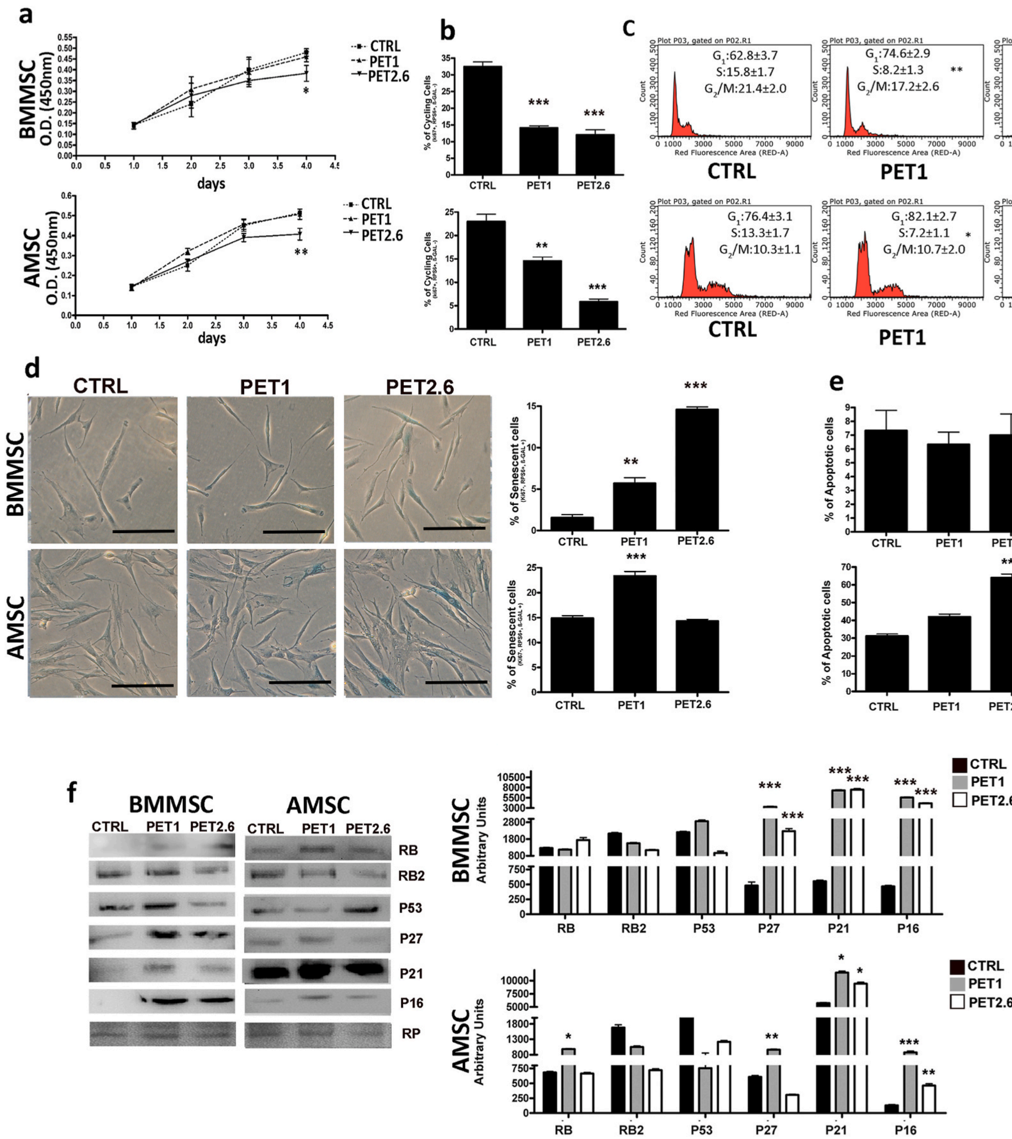

Fig. 1. -Biological properties of AMSCs and BMMSCs after treatments with PET1 and PET2.6 compared to control untreated cultures (CTRL) a – Cell proliferation measured by Cell Counting Kit-8,one, two and three days after treatments. ($n = 3 \pm SD$; $^*p < 0.05$, $^{**}p < 0.01$). b –Histograms show the percentage of cycling MSCs (Ki67+, pRPS6+, β-Gal-), after PET treatments ($n = 3 \pm SD$; $^{**}p < 0.01$, $^{***}p < 0.001$). c – The graphs show representative FACS analysis. Percentages of different cell populations (G1, S, and G2/M) are indicated ($n = 3 \pm SD$; $^*p < 0.05$, $^{**}p < 0.01$). d –Representative microscopic fields of senescence-associated beta-galactosidase–positive cells. On the right, histograms show the percentage of senescent MSCs (Ki67 -, pRPS6 +, β-Gal +). ($n = 3 \pm SD$; $^{**}p < 0.01$, $^{***}p < 0.001$). The black bar corresponds to 100 μm. e − Histograms show the percentage of apoptotic cells ($n = 3$, $\pm SD$; $^{***}p < 0.001$). f – Expression levels of proteins involved in senescence and/or apoptosis phenomena. Ponceau Red (RP) was used as a loading control. On the right, the histograms show the quantitative western blot analysis ($n = 3 \pm SD$; $^*p < 0.05$, $^{**}p < 0.01$, $^{***}p < 0.001$). . (For interpretation of the references to color in this figure legend, the reader is referred to the Web version of this article.)

3.3. *Effects of MPs-PET on MSC stemness*

Any stress may alter stem cell functions. In this context, we studied the MPs-PET effects on the properties of stem cells present in MSCs. In detail, we analyzed self-renewal and multipotentiality, which are fundamental for preserving the performance of a stem cell, i.e. contribution to tissue regeneration and organismal homeostasis. We carried out a CFU assay to check clonogenicity, which is a basic characteristic for stem cell self-renewal.

As showed in Figs. 3a and 4a, PET1 treatment induced a decrease in the number of CFUs in both AMSCs and BMMSCs, whereas PET2.6 showed a decrease only in AMSCs.

The differentiation potential of MSCs based on their spontaneous ability to be committed into adipocytes, osteocytes, and chondrocytes was assessed (Figs. 3b and 4b). We observed modifications in this capacity: the AMSCs showed a bias towardthe adipocytelineage specification in presence of PET1 and to lesser extent with PET2.6 (Fig. 4b), while BMMSCs showed a propensity to osteocytelineage commitment (Fig. 3b), associated with a decline in chondrocyte lineage specification (Fig. 3b).

We then determined the capacity of these cells to external cue-induced differentiation in adipocytes, osteocytes and chondrocytes. The results showed that, in presence of PET1 and PET2.67, AMSCs remained in an early stage of adipocyte differentiation as shown by the high levels of *PPARG* mRNA and the reduction in *LPL* mRNA, which are early and late differentiation markers, respectively (Fig. 4c). The PET1 and PET2.6 treatments induced a loss in osteocyte differentiation while the PET 2.6 impaired the chondrocyte differentiation. Similar results were observed in MPs-PET-treated BMMSC cultures with alteration of differentiation processes. In detail, PET1 and PET2.6 arrested osteocyte

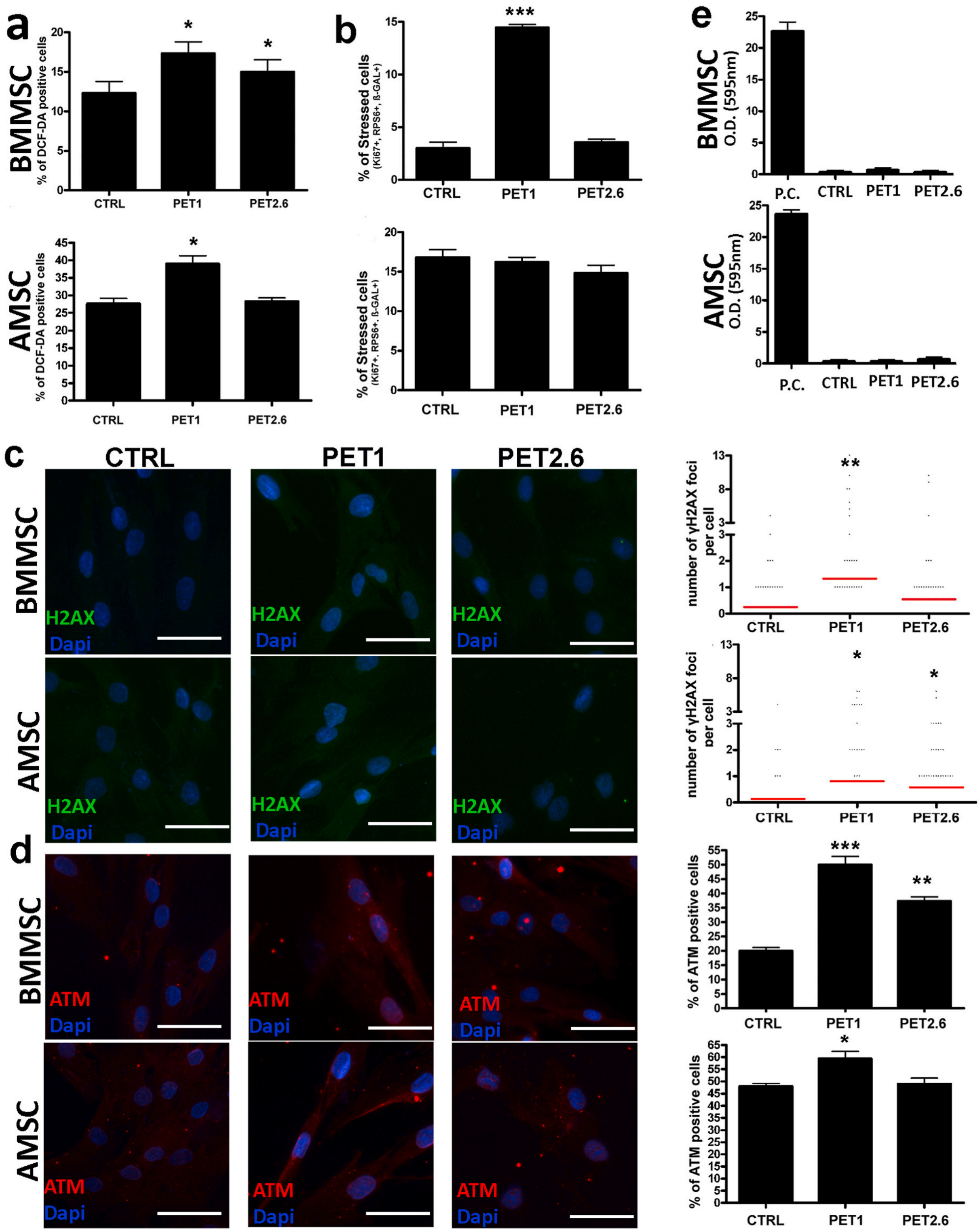

Fig. 2. Evaluation of DNA damage in AMSCs and BMMSCs after treatments with PET1 and PET2.6 compared to control untreated cultures (CTRL) a- The histograms show the percentage of DCF-DA positive cells (n = 3 ± SD; *p < 0.05). b –The histograms show the percentage of stressed MSCs (Ki67 +, pRPS6 +, β-Gal +). (n = 3 ± SD; ***p < 0.001). c -.Fluorescence images show the merge of cells stained with anti-γH2AX and nuclei stained with DAPI. On the right, graphs show the degree of γH2AX foci per cell (n = 3 ± SD; *p < 0.05 and **p < 0.01). d - Fluorescence images show typical cells stained with anti-ATM and nuclei stained with DAPI. On the right the histograms indicate the mean percentage of ATM-positive cells for each condition (n = 3 ± SD; *p < 0.05, **p < 0.01 and ***p < 0.001). e – Histograms show optical density readings at 595 nm obtained from methanol elution of the crystal violet stain for each condition (n = 3, ±SD). We used HEK-293 kidney embryonal cells as a positive control (PC). The scale bar represents 10 μm. (For interpretation of the references to color in this figure legend, the reader is referred to the Web version of this article.)

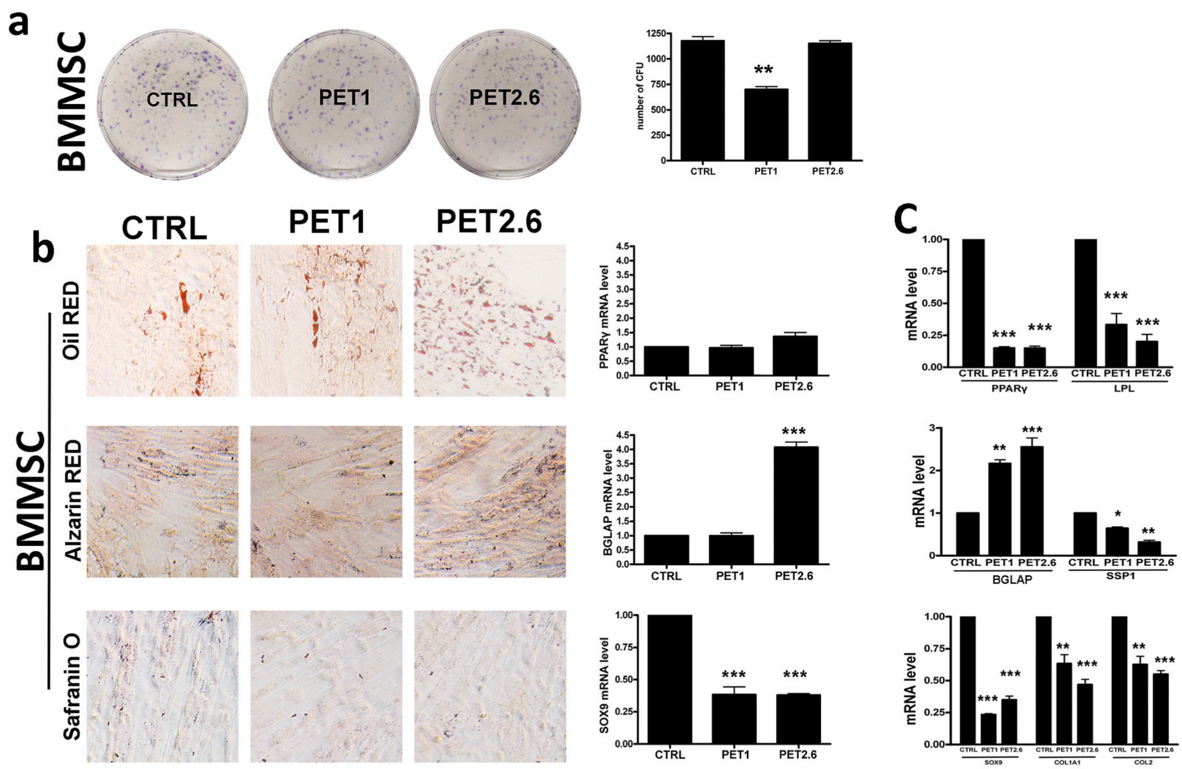

Fig. 3. Stemness properties of AMSCs and BMMSCs after treatments with MPs-PET1 and MPs-PET2.6 compared to control untreated cultures (CTRL) a – The pictures show representative crystal violet staining of clones. On the right, the histograms show the number of clones obtained (n = 3, ±SD; $^{**}p < 0.01$). b – Microscope images of differentiated cells: adipocyte (Oil RED), osteocyte (Alizarin RED) and chondrocyte (Safranin O). On the right, the histograms show mRNA levels of differentiation markers in spontaneous condition. GAPDH was selected as internal control (n = 3 ± SD; $^{***}p < 0.001$). c - The histograms show mRNA levels of differentiation markers in cue-differentiation. GAPDH was selected as internal control (n = 3 ± SD; $^{*}p < 0.05$, $^{**}p < 0.01$ and $^{***}p < 0.001$). (For interpretation of the references to color in this figure legend, the reader is referred to the Web version of this article.)

differentiation in a early stage, as evidenced by an increase in *BGLA* mRNA, associated with reduction of *SSP1* (early and late differentiation markers, respectively). Of note, the PET treatments significantly impaired the BMMSCs ability to differentiate into adipocytes and chondrocytes (Fig. 3c).

4. Discussion

Over the last years, MPs have increased in a variety of products, from water bottles to synthetic clothing, cosmetics and plastic bags. The toxicity of MPs also depends on the increased bioaccumulation potential that has rendered toxicological effects on the environment and also on human health through the food chain (Conti et al., 2020; Ferrante et al., 2021; Goodman et al., 2021; Geddings and Mackman., 2013; Childs et al., 2015). Not only, but also the shape and size of these MPs fall among the harmful aspects of these substances (Zitouni et al., 2021). For these reasons, detailed research is required to characterize these compounds and understand their effect on human health.

To better understand the effects of MPs on the fate of stem cells, we carried out several experiments with two different sizes of MPs-PET<1 and < 2.67 μm on MSCs present in the bone marrow. The presence of MSCs within all the organs and tissues that contain stroma prompted us also to studythe MSCs isolated from AT, where these cells may be more prone to MPs contamination than those present in the bone marrow. The MSC stem cells componentcan differentiate into adipocytes, osteocytes, and chondrocytes. MSCs locate in various tissues receive strong attention for their therapeutic capacities for these reasons represent a good study model (Squillaro et al., 2017).

Besides supporting hematopoiesis, the MSCscontribute to tissue renewal. They also sustain through paracrine effects, site-specific epithelial and endothelial responses, secrete growth factors and ECM proteins, and also display a local anti-inflammatory capability (Kruk et al., 2018).

The treatment of MSCs with MPs-PET significantly changed the fate of these cells. Indeed, after 3 days of treatment, we observed a significant decrease in the proliferation rate of MSCs isolated from both the BM and adipose tissue. Reduction of cycling cells could either indicate that cells entered quiescence or, alternatively, the MPs-PET may produce genotoxic damages, which trigger senescence or apoptosis. Thus, we assessed the percentage of senescent and apoptotic cells using the Senescence-Associated β -Galactosidase (SA -β-gal) and Annexin V assay, respectively. Some findings evidenced that SA -β-gal is highly active even after persistent stress, such as forced culture conditions, changes in temperature and pH values (Lee et al., 2006; Wood and Cavender, 2004). This event may limit the use of SA -β-gal as a senescence marker. The reduction of this proliferation was associated with the onset of senescence, as demonstrated by the acid β -galactosidase assay. The increase in senescence is in line with the reduction of the proliferation and signified that a single dose of MPs-PET could cause a negative effect in cells. Several papers, showed that the treatment with MPs-PET reduced the proliferation rate and the cell growth of different cell lines (Goodman et al., 2021).

The effects observed on the fate of these cells led us to focus on two important aspects that characterize stem cells: self-renewal and differentiation capacity. We carried out a CFU assay to test their clonogenicity, which is an important feature of self-renewing stem cells, as well as their differentiation into adipocytes, osteocytes and chondrocytes. We observed significant differences between control and MPs-PET-exposed cells, suggesting that MPs-PET may be dangerous to MSCs.

Several experiments showed that the exposure of living cells to MPs

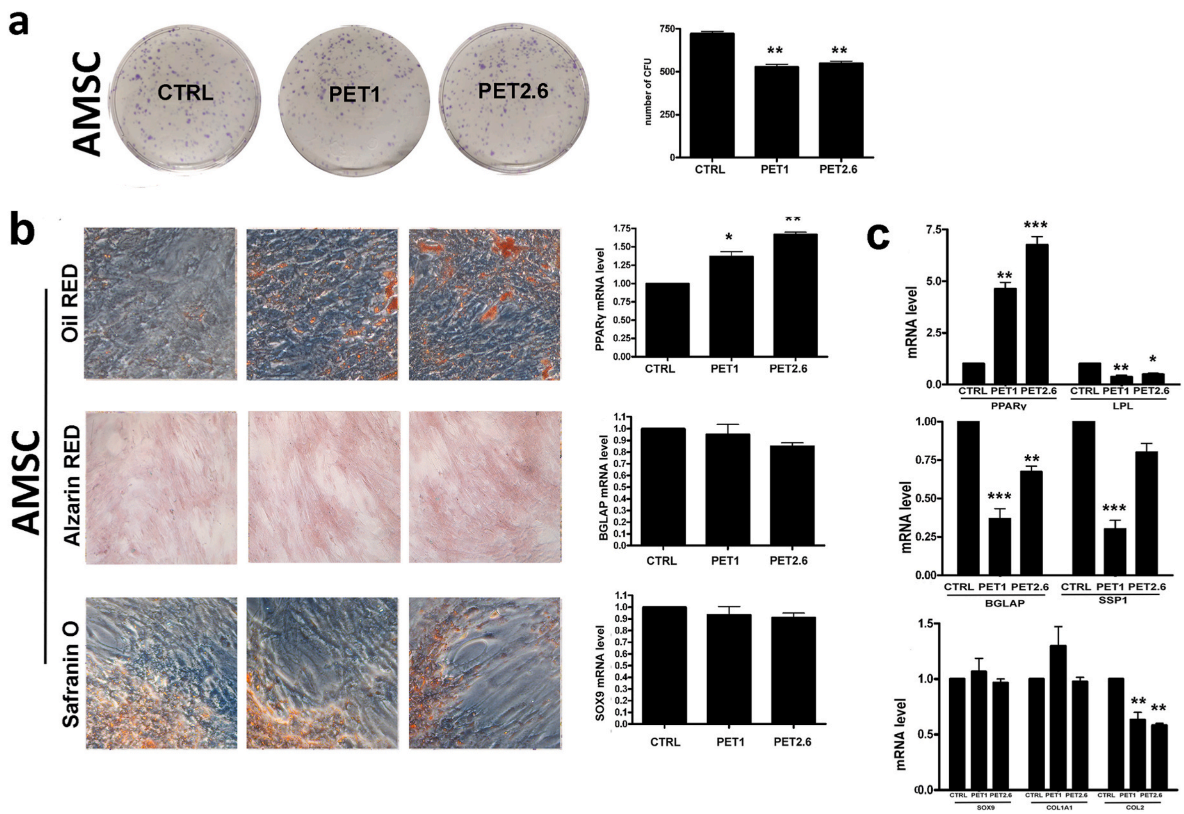

Fig. 4. Stemness properties of AMSCs after treatments with PET1 and PET2.6 compared to control untreated cultures (CTRL). a – The pictures show representative crystal violet staining of clones. On the right, the histograms show the number of clones obtained (n = 3, ± SD; ** p<0.01). b – Microscope images of differentiated cells: adipocyte (Oil RED), osteocyte (Alizarin RED) and chondrocyte (Safranin O). On the right, the histograms show mRNA levels of differentiation markers in spontaneous condition. GAPDH was selected as internal control (n = 3± SD;*** p<0.001). c - The histograms show mRNA levels of differentiation markers in cue-differentiation. GAPDH was selected as internal control (n = 3± SD;*p<0.05, **p<0.01 and *** p<0.001).

may cause the overproduction of free radicals, in particular ROS (Hamed et al., 2020; Vecchiotti et al., 2021). An excessive generation of ROS and their accumulation in cells cause oxidative stress, this increase induceshigher probability of cancer risk and/or senescence. Our study evidenced that MPs-PET exposure promoted ROS accumulation in MSCs inducing un-repaired DNA damage that triggers senescence. Increase in ROS was not detected in AMSCs treated with PET-2.67. This observation may be at odds with the other results, it must be underlined that the PET2.6 treatment induced apoptosis rather than senescence in AMSC, dead cells with high levels of intracellular ROS may detach from cell plates and hence ROS increase may be overlooked.

Indeed, at high levels, ROS can lead to impaired physiological function through cellular damage of DNA (Rowe et al., 2008). Un-repaired/mis-repaired DNA damages by evaluating the persistence of active H2AX (γ-H2AX) and ATM nuclear foci. Histone H2AX is an important regulator of cellular responses to DNA damage and is considered a hallmark of damaged DNA nuclear foci. ATM is a kinase that regulates DNA repair. Activation of ATM by autophosphorylation at Ser 1981 (pATM) signals the presence of DNA injury (Kobayashi et al., 2009). A correct DNA repair is achieved within a few hours from alteration, the permanence of pH2AX and pATM foci for hours or days following genotoxic events may indicates the presence of un-repaired/mis-repaired DNA damages, which can harm cell's physiological function by promoting either senescence or, alternatively, neoplastic transformation.

Senescence occurring in stem cell compartments, such as those hosting MSCs, are particular dangerous since any damage to stem cell pools may have profound consequences for human health. Indeed, MPs-PET-induced senescence of MSCs altered the self-renewal capacity of stem cells and undermine their differentiation potential (Childs et al., 2015).

Several studies claim that there are risks induced by EMPs-PET, specifically, an increase in the possibility of tumors (Geddings and Mackman., 2013). To ascertain whether MPs-PET had caused genetic changes to MSCs that would induce neoplastic changes, we carried out a soft agar assay, which demonstrated that the exposure of MSCs to EMPs-PET<1 μm and EMPs-PET<2.67 μm could not genetically modify MSCs, even when maintained in culture for an additional 21 days. These results do not exclude that MP long exposure time-periods and or cultivation for periods longer than 21 days may promote some neoplastic events.

5. Conclusion

In conclusion, our study revealed that MPs-PET exposure modified the fate of MSCs *in-vitro*, inducing senescence with the loss of several properties of stem cells. Our *in-vitro* study is innovative in demonstrating that there are significant changes in thebiology of MSCs after their exposure to MPsand NPs. This could pave the way to *in vivo* studies to evaluate effect of MPs on stem cell niches to evaluate which kinds of damages may affect stem cells following exposure to such potentially genotoxic agents.

Authors' contributions

NA, **HN**, and **TS** provided substantial contributions to conception and design, data acquisition and data analysis and interpretation; **NA**, **HN**, **GO**, **MF**, **MB**: Writing - original draft, Writing - review & editing, and critically revising it for important intellectual content; **GC**, **MF**, **GB**, **UG**, **IM**, **SM**, **MB**, they provided final approval of the version to be published; **NH**, **NA**, **TS**, **GC**, **MF**, **GB**, **UG**, **IM**, **SM**, **MB** are agreement to be accountable for all aspects of the work in ensuring that questions related to the accuracy and integrity of the work are appropriately investigated and resolved.

Declaration of competing interest

The authors declare that they have no known competing financial interests or personal relationships that could have appeared to influence the work reported in this paper.

Data availability

No data was used for the research described in the article.

Acknowledgement

This work was supported by funds from the Ministry of Higher Education, Tunisia, LR21AGR02.

References

Alessio, N., Capasso, S., Ferone, A., Di Bernardo, G., Cipollaro, M., Casale, F., Peluso, G., Giordano, A., Galderisi, U., 2017. Misidentified human gene functions with mouse models: the case of the retinoblastoma gene family in senescence. Neoplasia 19.
Alessio, N., Del Gaudio, S., Capasso, S., Di Bernardo, G., Cappabianca, S., Cipollaro, M., Peluso, G., Galderisi, U., 2015. Low dose radiation induced senescence of human mesenchymal stromal cells and impaired the autophagy process. Oncotarget. Apr 10 6 (10), 8155–8166.
Alessio, N., Pipino, C., Mandatori, D., Di Tomo, P., Ferone, A., Marchiso, M., Melone, M.A.B., Peluso, G., Pandolfi, A., Galderisi, U., 2018a. Mesenchymal stromal cells from amniotic fluid are less prone to senescence compared to those obtained from bone marrow: an in vitro study. J Cell Physiol 233.
Alessio, N., Riccitiello, F., Squillaro, T., Capasso, S., Del Gaudio, S., Di Bernardo, G., Cipollaro, M., Melone, M.A.B., Peluso, G., Galderisi, U., 2018b. Neural stem cells from a mouse model of Rett syndrome are prone to senescence, show reduced capacity to cope with genotoxic stress, and are impaired in the differentiation process. Exp Mol Med. Mar 22 (3), 50.
Alessio, N., Aprile, D., Cappabianca, S., Peluso, G., Di Bernardo, G., Galderisi, U., 2021. Different stages of quiescence, senescence, and cell stress identified by molecular algorithm based on the expression of Ki67, RPS6, and beta-galactosidase activity. International journal of molecular sciences 22.
Bredeck, G., Halamoda-Kenzaoui, B., Bogni, A., Lipsa, D., Bremer-Hoffmann, S., 2021. Tiered testing of micro- and nanoplastics using intestinal in vitro models to support hazard assessments. Environ. Int. 158, 106921.
Cappello, T., De Marco, G., Oliveri Conti, G., Giannetto, A., Ferrante, M., Mauceri, A., Maisano, M., 2021. Time-dependent metabolic disorders induced by short-term exposure to polystyrene microplastics in the Mediterranean mussel *Mytilus galloprovincialis*. Ecotoxicol Environ Saf. Feb 209, 111780.
Childs, B.G., Durik, M., Baker, D.J., van Deursen, J.M., 2015. Cellular senescence in aging and age-related disease: from mechanisms to therapy. Nat Med 21 (12), 1424–1435, 2015 Dec.
Conti, G.O., Ferrante, M., Banni, M., Favara, C., Nicolosi, I., Cristaldi, A., Fiore, M., Zuccarello, P., 2020. Micro-and nano-plastics in edible fruit and vegetables. The first diet risks assessment for the general population. Environ. Res. 187, 109677.
De Marco, G., Conti, G.O., Giannetto, A., Cappello, T., Galati, M., Iaria, C., Pulvirenti, E., Capparucci, F., Mauceri, A., Ferrante, M., Maisano, M., 2022. Embryotoxicity of polystyrene microplastics in zebrafish Danio rerio. Environ. Res. 208, 112552, 2022 May 15.
Ferrante, M., Pietro, Z., Allegui, C., Maria, F., Antonio, C., Pulvirenti, E., Favara, C., Chiara, C., Grasso, A., Omayma, M., et al., 2021. Microplastics in Fillets of Mediterranean Seafood. A Risk Assessment Study. Environmental research, 112247.
Fournier, E., Etienne-Mesmin, L., Grootaert, C., Jelsbak, L., Syberg, K., Blanquet-Diot, S., Mercier-Bonin, M., 2021. Microplastics in the human digestive environment: a focus on the potential and challenges facing in vitro gut model development. J. Hazard Mater. 415, 125632, 2021 Aug 5.
Galderisi, U., Giordano, A., 2014. The gap between the physiological and therapeutic roles of mesenchymal stem cells. Med. Res. Rev. 34, 1100–1126.
Geddings, J.E., Mackman, N., 2013. Tumor-derived tissue factor-positive microparticles and venous thrombosis in cancer patients. Blood 122 (11), 1873–1880, 2013 Sep. 12.
Goodman, K.E., Hare, J.T., Khamis, Z.I., Hua, T., Sang, Q.A., 2021. Exposure of human lung cells to polystyrene microplastics significantly retards cell proliferation and triggers morphological changes. Chem. Res. Toxicol. 34, 1069–1081.
Guerrera, M.C., Aragona, M., Porcino, C., Fazio, F., Laurà, R., Levanti, M., Montalbano, G., Germanà, G., Abbate, F., Germanà, A., 2021. Micro and nano plastics distribution in fish as model organisms: histopathology, blood response and bioaccumulation in different organs. Appl. Sci. 11, 5768.
Hamed, M., Soliman, H.A.M., Osman, A.G.M., Sayed, A.E.H., 2020. Antioxidants and molecular damage in Nile Tilapia (Oreochromis niloticus) after exposure to microplastics. Environ. Sci. Pollut. Res. Int. 27, 14581–14588.
Herold, J., Kalucka, J., 2020. Angiogenesis in adipose tissue: the interplay between adipose and endothelial cells. Front. Physiol. 11, 624903.
Jambeck, J.R., Geyer, R., Wilcox, C., Siegler, T.R., Perryman, M., Andrady, A., Narayan, R., Law, K.L., 2015. Marine pollution. Plastic waste inputs from land into the ocean. Science 347, 768–771.
Kannan, K., Vimalkumar, K., 2021. A review of human exposure to microplastics and insights into microplastics as obesogens. Front. Endocrinol. 12, 724989.
Kobayashi, J., Tauchi, H., Chen, B., Burma, S., Tashiro, S., Matsuura, S., Tanimoto, K., Chen, D.J., Komatsu, K., 2009. Histone H2AX participates the DNA damage-induced ATM activation through interaction with NBS1. Biochemical and biophysical research communications 380, 752–757.
Kruk, D., Heijink, I.H., Slebos, D.J., Timens, W., Ten Hacken, N.H., 2018. Mesenchymal stromal cells to regenerate emphysema: on the horizon? Respiration. international review of thoracic diseases 96, 148–158.
Lee, B.Y., Han, J.A., Im, J.S., Morrone, A., Johung, K., Goodwin, E.C., Kleijer, W.J., DiMaio, D., Hwang, E.S., 2006. Senescence-associated beta-galactosidase is lysosomal beta-galactosidase. Aging Cell 5, 187–195.
Leslie, H.A., Van Velzen, M.J.M., Brandsma, S.H., , DickVethaak, Garcia-Vallejo, J.J., Lamoree, M.H., 2022. Discovery and quantification of plastic particle pollution in human blood. Environ. Int. https://doi.org/10.1016/j.envint.2022.107199.
Missawi, O., Venditti, M., Cappello, T., Zitouni, N., Marco, G., Boughattas, I., Bousserrhine, N., Belbekhouche, S., Minucci, S., Maisano, M., Banni, M., 2022. Autophagic event and metabolomic disorders unveil cellular toxicity of environmental microplastics on marine polychaete Hediste diversicolor. Environ Pollut 302, 119106, 2022 Jun 1.
Oliveira, J., Belchior, A., da Silva, V.D., Rotter, A., Petrovski, Ž., Almeida, P.L., Lourenço, N.D., Gaudêncio, S.P., 2020. Marine environmental plastic pollution: mitigation by microorganism degradation and recycling valorization. Front. Mar. Sci. 7.
Oliveri Conti, G., Ferrante, M., Banni, M., Favara, C., Nicolosi, I., Cristaldi, A., Fiore, M., Zuccarello, P., 2020. Micro- and nano-plastics in edible fruit and vegetables. The first diet risks assessment for the general population. Environ. Res. 187, 109677.
Rowe, L.A., Degtyareva, N., Doetsch, P.W., 2008. DNA damage-induced reactive oxygen species (ROS) stress response in Saccharomyces cerevisiae. Free Radic. Biol. Med. 45 (8), 1167–1177, 2008 Oct 15.
Squillaro, T., Peluso, G., Galderisi, U., 2017. Clinical trials with mesenchymal stem cells: an update. Cell Transplant. 25 (5), 829–848, 2016.
Vecchiotti, G., Colafarina, S., Aloisi, M., Zarivi, O., Di Carlo, P., Poma, A., 2021. Genotoxicity and oxidative stress induction by polystyrene nanoparticles in the colorectal cancer cell line HCT116. PLoS One 16, e0255120.
Wood, M.A., Cavender, J.F., 2004. Beta-galactosidase staining as a marker of cells enduring stress. BIOS 75, 139–146.
Zitouni, N., Cappello, T., Missawi, O., Boughattas, I., De Marco, G., Belbekhouche, S., Mokni, M., Alphonse, V., Guerbej, H., Bousserrhine, N., Banni, M., 2022. Metabolomic disorders unveil hepatotoxicity of environmental microplastics in wild fish Serranus scriba (Linnaeus 1758). Sci. Total Environ. 10 (838), 155872. Pt 1.
Zitouni, N., Bousserrhine, N., Missawi, O., Boughattas, I., Chevre, N., Santos, R., Belbekhouche, S., Alphonse, V., Tisserand, F., Balmassiere, L., et al., 2021. Uptake, tissue distribution and toxicological effects of environmental microplastics in early juvenile fish Dicentrarchus labrax. J. Hazard Mater. 403, 124055.
Zuccarello, P., Ferrante, M., Cristaldi, A., Copat, C., Grasso, A., Sangregorio, D., Fiore, M., Oliveri Conti, G., 2019. Reply for comment on "Exposure to microplastics (<10 mum) associated to plastic bottles mineral water consumption: the first quantitative study by Zuccarello et al. [Water Research 157 (2019) 365-371]. Water Res. 166, 115077.